

The bacterial SRP receptor, FtsY, is activated on binding to the translocon

Albena Draycheva,¹ Thomas Bornemann,¹
Sergey Ryazanov,² Nils-Alexander Lakomek^{2,3*}
and Wolfgang Wintermeyer^{1*}

¹Department of Physical Biochemistry, Max Planck Institute for Biophysical Chemistry, Göttingen, Germany.

²Department of NMR-based Structural Biology, Max Planck Institute for Biophysical Chemistry, Göttingen, Germany.

³Department of Chemistry and Applied Biosciences, Laboratory of Physical Chemistry, Solid-state NMR, ETH Zürich, Zürich, Switzerland.

Summary

Proteins are inserted into the bacterial plasma membrane cotranslationally after translating ribosomes are targeted to the translocon in the membrane via the signal recognition particle (SRP) pathway. The targeting pathway involves an interaction between SRP and the SRP receptor, FtsY. Here we focus on the role of FtsY and its interaction with the translocon in controlling targeting. We show that in unbound FtsY the NG and A domains interact with one another. The interaction involves the membrane-targeting region at the junction between A and N domain. The closed form of FtsY is impaired in binding to SRP. Upon binding to the phospholipid-embedded translocon the domains of FtsY move apart. This enhances the docking of the FtsY NG domain to the homologous NG domain of the SRP protein Ffh. Thus, FtsY binding to the translocon has a central role in orchestrating the formation of a quaternary transfer complex in which the nascent peptide is transferred to the translocon. We propose that FtsY activation at the translocon ensures that ribosome–SRP complexes are directed to available translocons. This way sequestering SRP in futile complexes with unbound

FtsY can be avoided and efficient targeting to the translocon achieved.

Introduction

Cotranslational targeting of nascent membrane proteins to the endoplasmic reticulum of eukaryotic cells or the plasma membrane of bacteria is brought about by the signal recognition particle (SRP) pathway. SRP from *Escherichia coli* contains one protein, Ffh and 4.5S RNA (Bernstein *et al.*, 1993; Powers and Walter, 1997). SRP rapidly scans ribosomes until it settles on those exposing the signal peptide of a membrane protein and targets them to the protein-conducting channel (SecYEG in bacteria) in the membrane via an interaction with the SRP receptor, FtsY in bacteria (Halic *et al.*, 2006; Bornemann *et al.*, 2008; Holtkamp *et al.*, 2012; Jomaa *et al.*, 2016). The SecYEG translocon is a ternary complex consisting of proteins SecY, SecE and SecEg (Fig. 1A) that is integrated into the plasma membrane. Cryo-electron microscopic (cryo-EM) structures of bacterial SecYEG and the crystal structure of the homologous SecYE β from *Methanococcus jannaschii* show the translocon as a pseudosymmetrical structure with transmembrane (TM) segments 1–5 and 6–10 of SecY forming a central pore that in the resting state is closed by a small plug helix (Van den Berg *et al.*, 2004; Frauenfeld *et al.*, 2011; Park and Rapoport, 2012). For protein translocation through the translocon into the periplasm, the plug domain closing the pore toward the periplasm is moved to the side. Alternatively, to allow for TM segments of membrane proteins to enter the lipid phase, the two halves of the translocon move apart and open laterally.

FtsY is a peripheral membrane protein which interacts with membrane lipids and the translocon (Weiche *et al.*, 2008; Braig *et al.*, 2009; Mircheva *et al.*, 2009; Stjepanovic *et al.*, 2011) and has also been found in the cytoplasm (Luirink *et al.*, 1994). It is membrane-bound FtsY that promotes the release of SRP from the ribosome and the signal anchor sequence (SAS) (Valent *et al.*, 1998; Neumann-Haefelin *et al.*, 2000; Burk *et al.*, 2009; Mircheva *et al.*, 2009; Yosef *et al.*, 2010). FtsY from *E. coli*

Accepted 24 June, 2016. *For correspondences. E-mail wolfgang.wintermeyer@mpibpc.mpg.de; Tel. +49 5512012902; Fax +49 5512012905. E-mail nils-alexander.lakomek@phys.chem.ethz.ch; Tel. +41 44 632 4371; Fax +41 44 632 1621.

© 2016 The Authors. *Molecular Microbiology* Published by John Wiley & Sons Ltd.

This is an open access article under the terms of the Creative Commons Attribution-NonCommercial-NoDerivs License, which permits use and distribution in any medium, provided the original work is properly cited, the use is non-commercial and no modifications or adaptations are made.

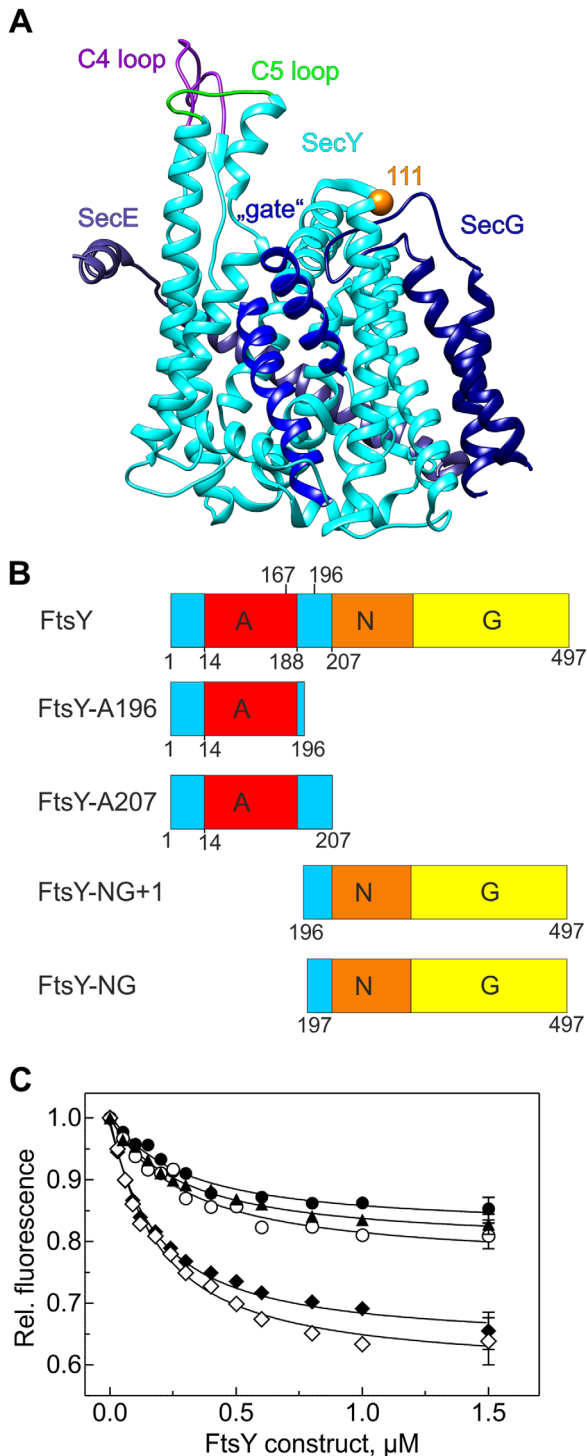


Fig. 1. Binding of FtsY and FtsY domains to SecYEG.

A. *E. coli* SecYEG structure (Park *et al.*, 2014) (PDB ID 3J45).

SecY, SecE, SecG and the cytoplasmic loops of SecY, C4 and C5, are indicated, as well as the lateral gate (blue) and position 111 where the MDCC fluorophore was attached (orange).

B. Domain structure of FtsY from *E. coli* and FtsY domain constructs. The A, N and G domains are colour-coded as indicated. FtsY-A196 and FtsY-A207 comprised 196 or 207 N-terminal amino acids of FtsY. The N-terminal lipid binding sequence and the membrane-targeting sequence (MTS) reaching up to residue 207 at the junction of A and NG domains are indicated in blue. The constructs FtsY-NG and FtsY-NG + 1 lacked the A domain and comprised residues 197–497 and 196–497 respectively.

C. Binding of full-length FtsY and FtsY domains to SecYEG. SecYEG(MDCC) (50 nM) was titrated with unlabelled FtsY (\blacktriangle), FtsY-NG + 1 (\circ), FtsY-NG (\diamond), FtsY-A196 (\blacklozenge) or FtsY-A207 (\bullet) monitoring MDCC fluorescence; for visual clarity representative error bars (SEM, $n = 2$) are depicted on the last titration point only. Fitting of the data (see “Experimental Procedures” section) yields a K_d value of $0.20 \pm 0.02 \mu\text{M}$ for FtsY and the four domain constructs.

disordered (Stjepanovic *et al.*, 2011; Lakomek *et al.*, 2016) and highly divergent in size among various prokaryotes (Bibi *et al.*, 2001; Haddad *et al.*, 2005). It preferentially binds to anionic phospholipids via two conserved membrane-binding sequences. These flank the A domain, one at the N terminus (amino acids 1–14), and a second, termed membrane targeting sequence (MTS) at the junction of A and N domains, which consists of amino acids 188–207 and is extended by helix N1 of the N domain (Stjepanovic *et al.*, 2011). Both amphiphilic sequences were reported to contribute to the lipid binding of FtsY and to be important for the membrane localization of FtsY (Weiche *et al.*, 2008; Braig *et al.*, 2009). The remainder of the A domain does not contribute significantly to the interaction with lipids (Braig *et al.*, 2009; Reinau *et al.*, 2010). While the A domain is responsible for the membrane localization of FtsY, the GTP-binding NG domain interacts with the homologous NG domain of SRP in a GTP-controlled manner to form the targeting complex (Kusters *et al.*, 1995; Egea *et al.*, 2004; Focia *et al.*, 2004; Shan *et al.*, 2004; Shan *et al.*, 2007; Zhang *et al.*, 2009; Jomaa *et al.*, 2016). The NG domain of FtsY alone (residues 197–497) does not support membrane insertion of proteins. However, the addition to the N-terminus of one more residue, Phe196, yields the FtsY-NG + 1 construct which *in vivo* is sufficient to support the growth of FtsY-depleted cells. When Phe196 is present, the short segment comprising residues 196–207, which is part of the longer MTS, assumes a helical structure which, due to its amphipathic character, can mediate membrane binding (Eitan and Bibi, 2004; Bahari *et al.*, 2007; Parltitz *et al.*, 2007).

At the membrane, FtsY interacts with the SecYEG translocon (Angelini *et al.*, 2005; 2006; Kuhn *et al.*, 2011). It approaches SecY from the side opposite the lateral gate and interacts with cytosolic loops 4 and 5

comprises three domains, the N-terminal A domain, the N domain and the C-terminal G domain; the latter two domains together form the functional NG domain (Bernstein *et al.*, 1989; Romisch *et al.*, 1989) (Fig. 1B). The highly acidic A domain tethers FtsY to the membrane (de Leeuw *et al.*, 1997; Zelazny *et al.*, 1997; Weiche *et al.*, 2008; Braig *et al.*, 2009). The A domain is intrinsically

(C4 and C5) via the A domain and, in part, the NG domain (Kuhn *et al.*, 2011; 2015). The cytosolic loops of SecY form the binding platform for other binding partners, such as the ribosome or SecA, the latter mediating posttranslational protein translocation in bacteria (Kudva *et al.*, 2013; Park and Rapoport, 2012).

In the present work we examine the interaction of FtsY and SecYEG in a quantitative manner, focusing on the contributions of A and NG domains of FtsY and rearrangements of the SecYEG–FtsY complex upon binding to ribosomes in the presence or absence of SRP. We monitor the fluorescence of labelled SecYEG to quantify the binding of FtsY or its isolated domains. To monitor rearrangements of the A and NG domains of FtsY on binding to SecYEG and SRP we perform FRET measurements, two-dimensional NMR spectroscopy on isotope-labelled FtsY, and site-directed crosslinking. To handle SecYEG in monomeric, biochemically defined form we use SecYEG embedded in nanodiscs, discoidal phospholipid bilayers held together by two copies of membrane scaffold protein (MSP1D1) derived from apolipoprotein A1 (Denisov *et al.*, 2004; Alami *et al.*, 2007; Ge *et al.*, 2014). Nanodiscs have proven to be effective in solubilizing membrane proteins and have been used to study a wide variety of membrane proteins, including SecYEG (Alami *et al.*, 2007; Kedrov *et al.*, 2013; Ge *et al.*, 2014).

Results

Interaction of FtsY domains with the SecYEG translocon

To assess the contributions of the A and NG domains of FtsY to complex formation with the translocon we perform equilibrium titrations with the SecYEG translocon embedded into *E. coli* phospholipids contained in nanodiscs (see “Experimental Procedures” section), monitoring the fluorescence of the MDCC fluorophore at position 111 in the cytosolic side of TM3 of SecY (Fig. 1A), which is distant from the binding sites of FtsY and ribosomes (Kuhn *et al.*, 2011). We examine the binding of the FtsY-NG and NG + 1 domains as well as that of the FtsY-A196 and FtsY-A207 domains (Fig. 1B). The two NG domain constructs are well-studied variants; while both constructs bind GTP or GDP with affinities comparable to that of FtsY, interact with SRP, and enhance the GTPase activity of the complex, only the NG + 1 construct is active in membrane targeting *in vivo* (Bahari *et al.*, 2007). The other two domain constructs are variants of the A domain, comprising the N-terminal 196 or 207 amino acids of FtsY. The smaller construct, FtsY-A196, contains an amphiphilic sequence (residues 1–14) at the N terminus and part of the MTS (residues 188–196) at the C terminus, whereas FtsY-A207

contains the complete MTS formed of residues 188–207 (Stjepanovic *et al.*, 2011) at the C terminus, allowing to examine the role of the MTS in the interaction of FtsY with SecYEG and phospholipids of the membrane. Complex formation with SecYEG is monitored by the decrease of MDCC fluorescence, which is larger for the two NG domain constructs than for the A domain constructs. The titrations yield K_d values around 0.2 μM for all four domain variants and full-length FtsY (Fig. 1C).

Translocon binding of unlabelled full-length FtsY (Fig. 1C) has about the same K_d value of $0.18 \pm 0.02 \mu\text{M}$ as previously determined with fluorescence-labelled FtsY (Kuhn *et al.*, 2015). The MDCC label on SecY does not affect complex formation as well, as fluorescence-labelled FtsY binds to the unlabelled translocon with the same affinity (Kuhn *et al.*, 2015). Furthermore, the function of the translocon in binding a ribosome-nascent-chain complex (RNC) and protecting the N-terminal signal anchor sequence against proteolysis is not impaired by the MDCC label at position 111 (Supporting Information Fig. S1). Our previous results also showed that FtsY binds to SecYEG only when it is surrounded by phospholipids, as complex formation is not observed with SecYEG solubilized by adding detergent (Kuhn *et al.*, 2015). FtsY binding to empty lipid nanodiscs is much weaker ($K_d = 1.2 \mu\text{M}$) (Kuhn *et al.*, 2015), indicating that the affinity of the complex of FtsY with SecYEG embedded in a phospholipid bilayer is governed by the electrostatic interaction of FtsY with SecY (Lakomek *et al.*, 2016), although there may be a contribution of anionic phospholipids, which are accumulated around the translocon (Prabudiansyah *et al.*, 2015). An enrichment of anionic phospholipids we observe for nanodiscs containing SecYEG, as well (see “Experimental Procedures” section).

Interestingly, full-length FtsY binds with the same affinity as either isolated domain, rather than with the combined affinities of the domains, as one might expect assuming that the two domains bind independently. One possibility to explain this behaviour would be that the domains bind to SecYEG or phospholipids in an anti-cooperative manner, impairing one another's binding. Alternatively, unbound FtsY could be present in a non-binding conformation that has to rearrange to allow for complex formation with SecYEG, and that the energy required for the rearrangement consumes (part of) the free energy of binding of either domain, resulting in a lower apparent binding affinity of the full-length protein. To distinguish the two models we performed the following experiments.

Interaction between the A and NG domains of FtsY

We first examined whether the isolated A and NG domains can bind simultaneously to SecYEG,

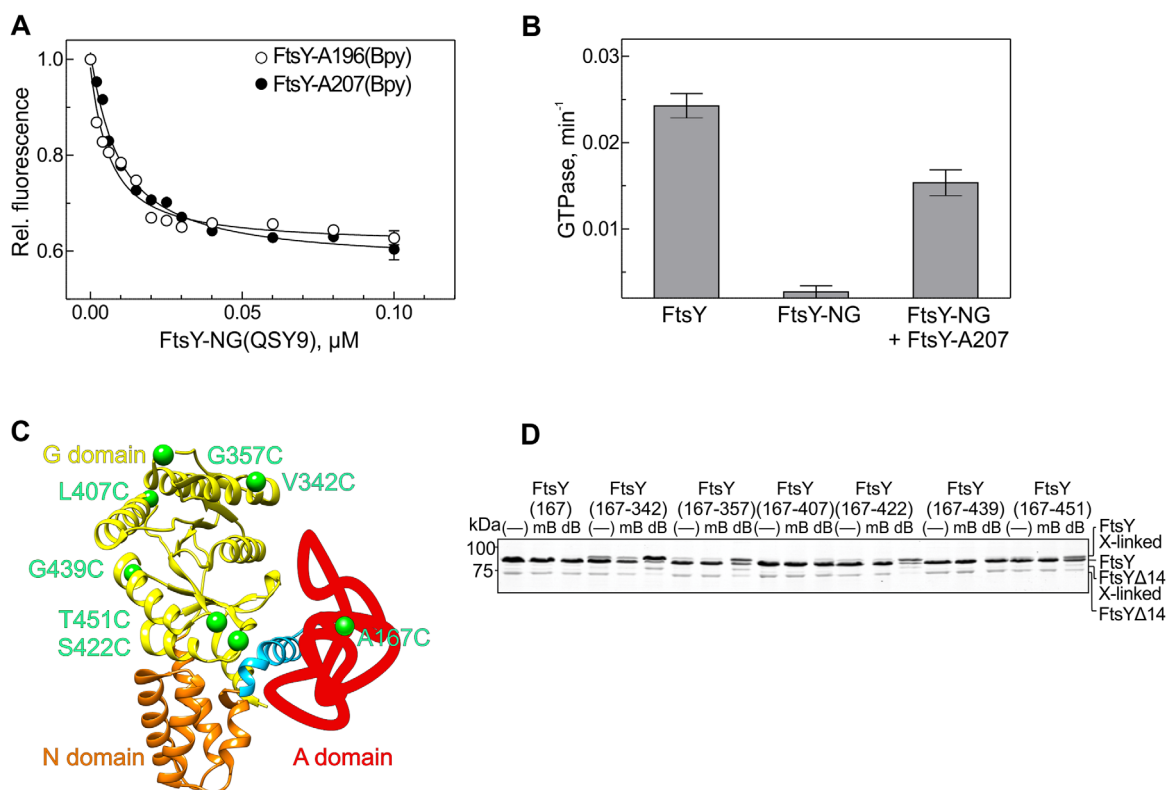


Fig. 2. Association of FtsY-A and FtsY-NG domains.

A. Fluorescence titrations. FtsY-A196 (○) or FtsY-A207 (●) (2 nM) labelled with Bpy at position A167C (donor) were titrated with FtsY-NG labelled with the non-fluorescent FRET acceptor QSY9 at position V342C. Bpy fluorescence is plotted relative to the initial fluorescence measured prior to the addition of NG domain. Representative error bars (SEM, $n = 2$) are shown for the last titration point only. Fitting the data (see “Experimental Procedures” section) yields $K_d = 10 \pm 4$ nM.

B. GTPase activation of FtsY-NG by FtsY-A. The GTPase activity of FtsY or FtsY-NG was determined with [γ - 32 P]GTP (see “Experimental Procedures” section) and compared with the activity of FtsY-NG measured in the presence of FtsY-A207; error bars represent SD ($n = 3$).

C. Positions of cysteine residues engineered into the G domain for chemical crosslinking with C167 in the A domain (arbitrary red line). The structure of the NG domain is from (Stjepanovic *et al.*, 2011) (PDB: 2YHS). The MTS (residues 188–207) at the junction of A and N domains is indicated in blue.

D. FtsY interdomain crosslinks. The interaction between the A and G domains of FtsY containing two cysteine residues at the positions indicated in (C) was probed by dibromobimane (dB), and the products were resolved on a 12% Tris-Glycine denaturing gel. Crosslinking lowered the electrophoretic mobility of FtsY or truncated FtsY Δ 14 (faint band at ~70 kD). Controls were performed with monobromobimane (mB), or with dB and FtsY containing a single cysteine residue (C167), or in the absence of modifying reagent (–).

monitoring the binding of FtsY-A207 labelled with Bpy at position 167 to SecYEG(MDCC) in the absence or presence of saturating amounts (10 times K_d) of FtsY-NG (Supporting Information Fig. S2). The binding of the A domain to SecYEG is not changed significantly ($K_d \approx 0.2 \mu\text{M}$) in the presence of the NG domain, indicating that the domains bind independent of one another and occupy distinct binding sites on SecY. This excludes anti-cooperative binding of the FtsY domains to SecYEG and supports the alternative model featuring an intramolecular domain–domain interaction in FtsY. Indeed, the isolated A and NG domains form a high-affinity complex, as demonstrated by titrations monitored by FRET between a Bpy label at position 167 in the FtsY-A196/207 constructs and the non-fluorescent acceptor QSY9 at position 342 in the NG domain (Fig. 2A). For the two A-domain constructs, FtsY-A196 and FtsY-A207, the

titrations yield a K_d of around 10 nM for the complex with the NG domain.

Binding of the A domain to the NG domain can also be demonstrated by monitoring the GTPase activity of the NG domain. Full-length FtsY exhibits a low GTPase activity, about 0.025 min^{-1} (Fig. 2B), which is comparable to previously reported values (Peluso *et al.*, 2001; Akopian *et al.*, 2013). The activity is decreased about 10-fold in the isolated NG domain and increases about five-fold upon addition of a saturating amount of the A domain, providing evidence for an interaction between A and NG domains. Previously, the GTPase activity of full-length FtsY and of FtsY-NG were compared and a small inhibitory, rather than stimulatory effect of the A domain was observed (de Leeuw *et al.*, 2000). The difference between those data and ours, which is small in absolute terms, may be attributed to the use of different assay conditions and FtsY domain constructs.

To examine whether A and NG domains interact in full-length FtsY, we performed crosslinking experiments with di-bromobimane (dB), a thiol-specific bifunctional crosslinker which can crosslink cysteine residues that are 3–6 Å apart (Mornet *et al.*, 1985; Buskiewicz *et al.*, 2005). The structure of full-length FtsY and, therefore, the position of the A domain relative to the NG domain, is not known. To find suitable positions for crosslinking, we replaced several non-conserved residues in the G domain and position 167 in the A domain with cysteine (Fig. 2C). Upon reaction with dB, several of the di-substituted cysteine derivatives of full-length FtsY change their mobility in SDS gels (Fig. 2D). Truncated FtsY (FtsY Δ 14) lacking 14 N-terminal amino acids, which is usually present in FtsY preparations and was present in trace amounts in the preparation used here, is retarded as well (Weiche *et al.*, 2008). No shift is observed with FtsY(C167–C407) and FtsY(C167–C439). The mobility change is due to crosslinking, as the respective control reactions of either dB with mono-substituted FtsY(C167) or of mono-functional mono-bromobimane (mB) and the di-substituted FtsY(Cys)₂ derivatives do not change the mobility (Fig. 2D). The extent of crosslinking reaches up to about 50%–60%. The observation of short-distance crosslinks between position 167 in the A domain and a number of positions in the G domain (Fig. 2D), except positions 407 and 439, provides strong support for an interaction between the domains in intact FtsY and suggests that the A domain approaches the G domain from the side where the crosslinking positions are located (Fig. 2C).

The lack of structural information on the A domain does not allow for a precise estimation of the position of residue 167 relative to the crosslinked positions in the G domain. Nevertheless an approximation based on the cysteine-substituted positions in the G domain and the length of the crosslinker suggests that the cysteine residue in the A domain should sample distances of 5–6 Å to be in crosslinking range, consistent with intrinsic disorder of the A domain (Stjepanovic *et al.*, 2011). The lack of crosslinks with cysteines at positions 407 and 439 of the G domain (Fig. 2C, D), indicates a larger distance between those positions and position 167, and suggests that the crosslinking cysteine positions in the G domain outline the interface for the binding of the A domain.

NMR spectroscopy defines interaction site in the MTS

To localize the region of FtsY-A207 that is involved in the interaction with the NG domain, we have used solution NMR spectroscopy. The comparison of the spectra of isotope-enriched (²H, ¹⁵N, ¹³C) FtsY and FtsY-A207 (Supporting Information Fig. S3) reveals that only the A domain is visible by NMR. Apparently, due to its

intrinsically disordered nature (Stjepanovic *et al.*, 2011), the A domain is highly flexible, leading to favourable relaxation properties and narrow line widths. By contrast, the globular, folded NG domain is less flexible and not visible in the NMR spectra, presumably due to slow overall tumbling under the conditions of the measurements. Notably, we observe significant line-broadening in the ¹⁵N dimension for the entire A domain in full-length FtsY, compared with isolated FtsY-A207 (Supporting Information Fig. S3). This is attributed to the substantially larger molecular weight of full-length FtsY, compared with the A domain alone. The observed line broadening indicates that the NMR relaxation properties of the NG domain upon complex formation are passed on to the A domain, resulting in a less populated bound conformation and a highly populated free conformation of the A domain which are in fast exchange.

The spectral resonances can be assigned to individual amino acids in FtsY-A207, as described elsewhere (Lakomek *et al.*, 2016). Briefly, about 180 out of 190 expected resonances (207 amino acids minus 16 invisible proline residues and the invisible N-terminal amino acid) are visible in two-dimensional ¹⁵N¹H-TROSY-HSQC spectra of FtsY-A207; the remaining resonances either are hidden by spectral overlap or broadened below the detection threshold as the result of dynamic processes on the micro- to millisecond time scale. Out of the visible resonances, 110 could be assigned. Further assignments were precluded due to the high abundance of glutamic acid (25%), the presence of repetitive sequences, and close to random-coil chemical shifts. Nevertheless, the assigned resonances cover practically the entire A domain, leaving unassigned only small regions encompassing residues 30–50, 170–182, and 198–207.

To characterize the interactions between A and NG domains further, we recorded NMR spectra of isotope-labelled FtsY-A207 alone or in a complex with the NG domain. The addition of the NG domain does not change the spectrum appreciably, in that resonances are not shifted. However, the comparison of resonance intensities (Fig. 3) reveals that complex formation with the NG domain causes a substantial intensity decrease of several resonances in the region of residues 188–197 at the C terminus of the FtsY-A207 construct, indicating that the MTS is involved in binding to the NG domain. The NG-bound conformation of the MTS region is in slow exchange with the conformation of the unbound domain, which is visible in the NMR spectrum. In the spectra of full-length FtsY, in which the domains are linked together, resonances of residues 185–207 are invisible, suggesting that the equilibrium is shifted further to the bound (invisible) conformation.

Additionally, binding to the NG domain increases the intensities of several resonances of the A domain,

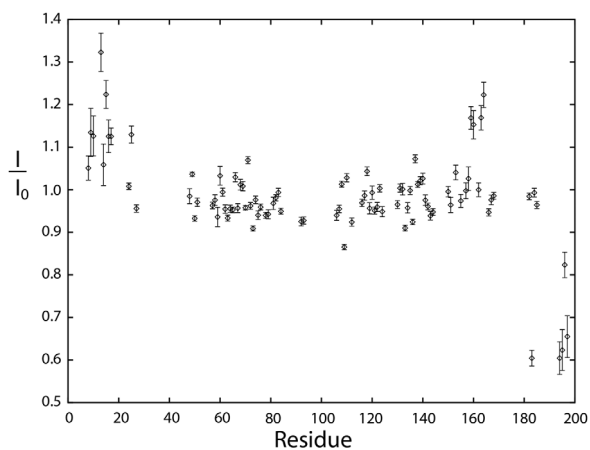


Fig. 3. Interaction of FtsY-A207 and FtsY-NG domains monitored by NMR. Two-dimensional NMR spectra (TROSY-HSQC) of $^2\text{H}/^{15}\text{N}/^{13}\text{C}$ -labelled FtsY-A207 were measured in the absence (I_0) and presence (I) of an equimolar amount of unlabelled FtsY-NG domain (see “Experimental Procedures” section). Plotted is the ratio of the intensities, I/I_0 , of assigned resonances (Lakomek *et al.*, 2016).

corresponding to residues located near the N terminus and residues around amino acid 159 (Fig. 3). Both regions show increased secondary structure propensity in the isolated A domain (Lakomek *et al.*, 2016), but appear more flexible and more disordered when the A domain is bound to the NG domain. This can be explained by an allosteric effect between binding regions of the A domain and regions with low population of pre-formed secondary structure. The NMR spectra indicate that the MTS plays an important role in the interaction with the NG domain, in accordance with the arrangement of the MTS and the N1 helix of the N domain observed in the crystal structure of FtsY (Stjepanovic *et al.*, 2011) (Fig. 2C).

NG and A domains move apart upon FtsY binding to SecYEG

Next we examined whether the interaction between A and NG domains observed for unbound FtsY is disrupted upon complex formation with SecYEG embedded in phospholipids. The rearrangement can be monitored by FRET between two Bpy fluorophores located at positions 167 in the A domain and 342 in the G domain. FRET between two identical fluorophores (“homo-FRET”) is detected by the lower fluorescence anisotropy of double-labelled compared with single-labelled protein (Runnels and Scarlata, 1995), as we have previously used to study domain–domain rearrangements in the SRP protein Ffh (Buskiewicz *et al.*, 2005). Double-labelled FtsY(Bpy) $_2$ exhibits a rather low anisotropy, compared with the average anisotropy of the equimolar mixture of the two single-labelled FtsY constructs used as control (Fig. 4). This indicates that the labels in G

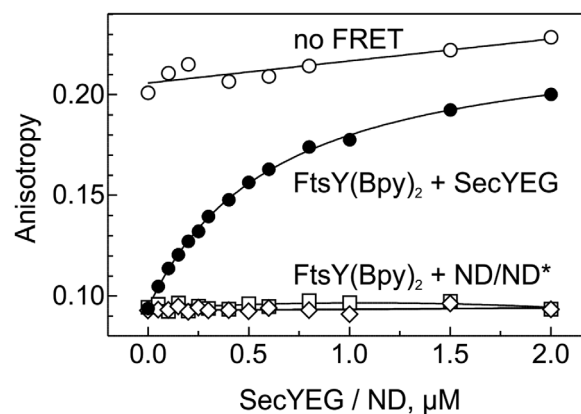


Fig. 4. FtsY domain rearrangement on binding to SecYEG. The rearrangement of the A and NG domains of FtsY was monitored by homo-FRET between Bpy labels at positions 167 in the A domain and 342 in the G domain (FtsY(Bpy) $_2$). FtsY(Bpy) $_2$ (50 nM) was titrated with nanodisc-embedded SecYEG (●) and fluorescence anisotropy was monitored. The fit of the data (see “Experimental Procedures” section) yields $K_d = 0.6 \pm 0.2 \mu\text{M}$ for FtsY(Bpy) $_2$ binding to SecYEG. The no-FRET control titration with SecYEG was performed with an equimolar mixture of single-labelled FtsY(Bpy167) and FtsY(Bpy342) (○). Further controls were performed with double-labelled FtsY(Bpy) $_2$ and empty nanodiscs with lower (ND, □) or higher (ND*, ◇) content of PG (see “Experimental Procedures” section). Error margins (SEM, $n = 2$) are smaller than the symbols.

and A domains of unbound FtsY are in close proximity, resulting in low anisotropy due to homo-FRET. Upon titration with SecYEG, the anisotropy of double-labelled FtsY is increased substantially, which indicates that the two Bpy labels come apart upon binding to SecYEG (Fig. 4), implying that the FtsY domains separate upon forming the complex. Consistent with this interpretation, in the control measurement with the mixture of the two single-labelled FtsY derivatives and SecYEG the anisotropy change is very small, which shows that the anisotropy increase observed with double-labelled FtsY is not caused by the increase of the molecular weight due to complex formation. The addition of empty nanodiscs with lower (ND) or higher (ND*) content of the anionic phosphatidylglycerol has no effect on the anisotropy of double-labelled FtsY (Fig. 4). Thus, FtsY binding to phospholipids alone does not induce the separation of NG and A domains. The SecYEG–FtsY(Bpy) $_2$ complex has a K_d of $0.6 \mu\text{M}$, compared with about $0.2 \mu\text{M}$ observed with unlabelled or single-labelled FtsY (Fig. 1C), suggesting that the interaction is only slightly impaired by introducing the second Bpy label.

Domain separation in FtsY is required for complex formation with SRP

A moderate increase of the anisotropy is also observed when SRP is bound to double-labelled FtsY in the

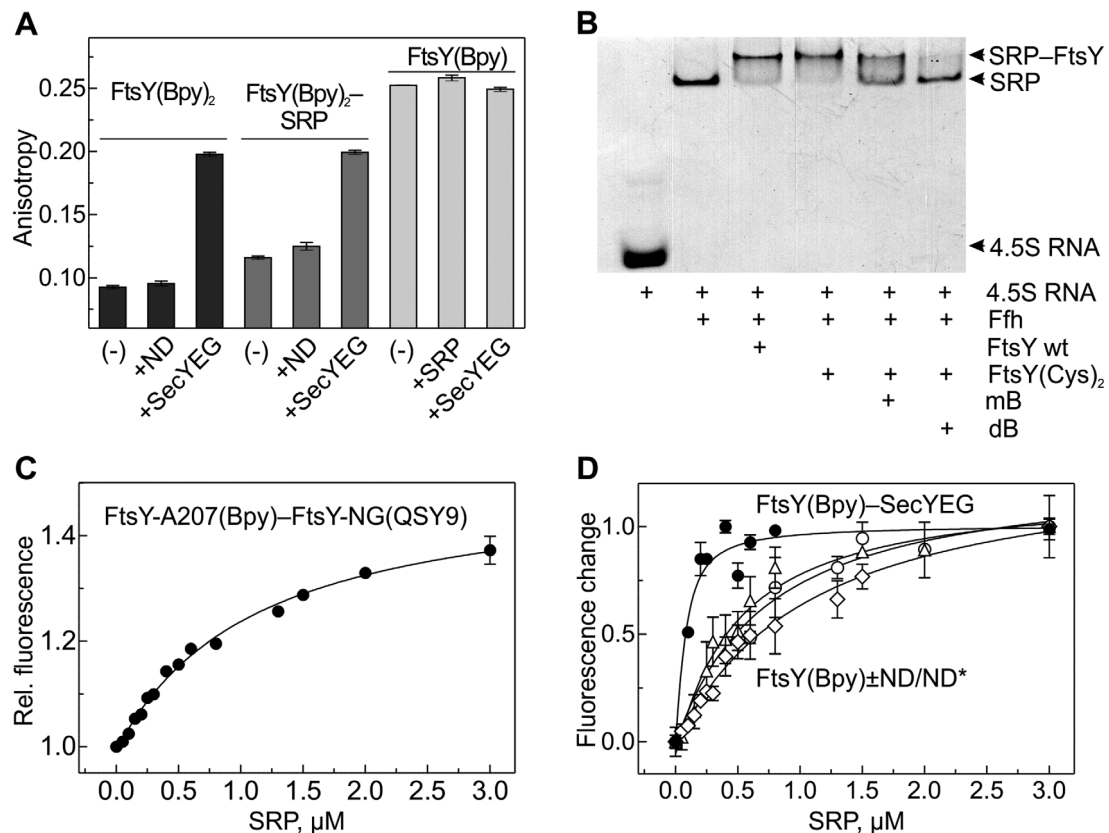


Fig. 5. FtsY domain rearrangement on binding SRP and SecYEG.

A. Domain rearrangement of FtsY(Bpy)₂ monitored by anisotropy. The fluorescence anisotropy of FtsY(Bpy)₂ alone was monitored upon addition of empty nanodiscs (ND) or SecYEG in nanodiscs (SecYEG) as in Fig. 4 (black columns) or in the presence of SRP (3 μ M; dark grey columns). Control measurements were carried out with single-labelled FtsY(Bpy342) (light grey columns).

B. Complex formation of SRP and FtsY as analyzed by mobility shift in native gel electrophoresis. The mobility shift of the 4.5S RNA was monitored upon formation of SRP and upon binding of SRP to FtsY (see ‘‘Experimental Procedures’’ section) using FtsY(Cys)₂ crosslinked with dB (cf. Fig. 2D), wt FtsY, or FtsY(Cys)₂ reacted with mB.

C. Dissociation of the complex of FtsY-A207 and FtsY-NG upon binding of SRP. The complex of FtsY-A207(Bpy167) and FtsY-NG(QSY342) (70 nM each) was titrated with SRP, monitoring the fluorescence increase of the Bpy donor due to reduced FRET. The titration was evaluated by nonlinear fitting (see ‘‘Experimental Procedures’’ section), yielding $K_d = 1.2 \pm 0.2 \mu$ M; error margins are SEM (n = 2).

D. Affinity of SRP–FtsY complex formation in the absence or presence of SecYEG or nanodiscs. FtsY labelled at position V342C with Bpy (FtsY(Bpy)) (70 nM) was titrated with SRP without addition (○) or in the presence of 7 μ M ND (△), ND* (◇), or of 1.5 μ M SecYEG in nanodiscs (●), monitoring the change in Bpy fluorescence. The titrations were evaluated as in (C), yielding the K_d values given in the text.

absence of SecYEG (Fig. 5A), and no such effect is seen with single-labelled FtsY. This suggests that SRP binding is accompanied by a movement of the A and NG domains of FtsY, which is, however, less extensive than that induced by SecYEG/phospholipid binding. The effects of SRP and SecYEG binding are not additive (compare the columns FtsY(Bpy)₂ + SecYEG \pm SRP in Fig. 5A), which indicates that binding to SecYEG already induces maximum domain separation in FtsY.

Bimane crosslinking of NG and A domains of the double-cysteine mutants of FtsY is highly efficient, in particular with FtsY(C167–C342) (> 60%; Fig. 2D). Using this crosslinked material, we examined complex formation with SRP by an established gel-mobility assay (Jagath *et al.*, 2000). The electrophoretic mobility of

4.5S RNA is strongly reduced by binding Ffh, indicating SRP formation, and SRP migration is retarded further when FtsY is added, indicating SRP–FtsY complex formation (Fig. 5B). The latter mobility shift is strongly inhibited when dB-crosslinked FtsY is used, while the control with mB shows a much smaller effect. This result indicates that separation of the A and NG domains in FtsY enhances the propensity of FtsY to bind SRP.

To examine the effect of SRP binding on the interaction of the FtsY domains further, we have used the complex of the FtsY domains, FtsY-A207 labelled with Bpy as FRET donor and FtsY-NG labelled in the G domain with the non-fluorescent FRET acceptor QSY9, to monitor SRP-induced domain rearrangements (Fig. 5C). Upon adding increasing amounts of SRP, a 40%

increase in donor fluorescence is observed at saturation, indicating a decrease in FRET efficiency. This is consistent with the A and G domains of FtsY moving apart upon binding SRP, and the 40% fluorescence increase matches the decrease of donor fluorescence due to FRET observed upon formation of the complex of the labelled domains (Fig. 2A). The K_d of SRP binding, $\approx 1.3 \mu\text{M}$, is comparable to the K_d of $0.7 \mu\text{M}$ for the complex of SRP with full-length FtsY (Fig. 5D). This K_d value is consistent with a value obtained previously under similar experimental conditions (Holtkamp *et al.*, 2012) and higher than the value reported for N-terminally truncated FtsY (Peluso *et al.*, 2000). These results suggest that the domain–domain interaction is similar in intact FtsY and the complex of the isolated domains.

Compared with the K_d of the binary SRP–FtsY complex ($K_d = 0.7 \pm 0.2 \mu\text{M}$), SRP binding to FtsY is strongly enhanced ($K_d = 0.05 \pm 0.01 \mu\text{M}$) when FtsY is bound to SecYEG in nanodiscs (Fig. 5D), whereas FtsY binding to empty nanodiscs with lower (ND) or higher (ND*) content of phosphatidylglycerol has no stabilizing effect, K_d remaining at $0.7 \pm 0.2 \mu\text{M}$. Thus, working with nanodiscs we do not observe the enhancement of FtsY–SRP complex formation reported for liposomes with high content of anionic phospholipids (Lam *et al.*, 2010). Our results suggest that the domain–domain separation is mainly induced by FtsY binding to SecYEG and exposes the FtsY-NG domain for binding to the NG domain of Ffh in SRP, thereby enhancing complex formation.

Concurrent binding of FtsY and ribosomes to the SecYEG translocon

Finally we wanted to verify whether FtsY can stay bound to the translocon upon binding of ribosomes, as observed earlier (Kuhn *et al.*, 2015), and which domain of FtsY facilitates complex formation. Thus, we have extended previous experiments performed with FtsQ-RNC (Kuhn *et al.*, 2015) and titrated SecYEG(MDCC) with FtsY labelled with Bpy at position 196 in the presence of vacant 70S ribosomes or Lep75/94-RNCs (ribosome-nascent-chain complexes carrying 75 or 94 N-terminal amino acids of leader peptidase) at increasing concentrations, monitoring the fluorescence change of MDCC due to FRET (Fig. 6). The control titration without added ribosomes yields a K_d value of about $0.2 \mu\text{M}$, that is the same as with unlabelled FtsY (Fig. 1C), indicating that the Bpy label does not influence complex formation. In all three cases the extent of the fluorescence change due to SecYEG–FtsY complex formation at saturation with ribosomes or RNCs is diminished, to about 20% with vacant ribosomes (Fig.

6A) and to about 10% with Lep-RNCs (Fig. 6B,C). The reduction of the FRET amplitudes (summarized in Fig. 6D) is not due to binding competition, because the apparent K_d values do not increase, as would be expected for competitive binding, and rather remain at $0.2 \pm 0.1 \mu\text{M}$ throughout the titrations. This indicates that ribosomes and FtsY bind to SecYEG in a non-competitive manner. On the other hand, the reduction of the FRET amplitude, which is indicative of an increased distance between donor and acceptor, shows that the arrangement of FtsY on SecYEG in the ternary complexes with ribosomes differs from the one in the binary complex, and that the difference is larger with the RNCs.

From the dependence of the FRET amplitudes on ribosome/RNC concentration (Fig. 6D), the apparent K_d of SecYEG binding to non-translating ribosomes, Lep75-RNC, or Lep94-RNC in the presence of FtsY is estimated to 10–20 nM. These values are in the same order as the ones obtained previously with FtsQ-RNCs (Kuhn *et al.*, 2015) and for the binary ribosome–SecYEG complexes formed in the absence of FtsY (Wu *et al.*, 2012; Ge *et al.*, 2014), in keeping with the observed lack of competition between FtsY and ribosomes in binding to SecYEG.

We performed analogous experiments with labelled ribosomes and FtsY or isolated FtsY domains, monitoring complex formation by FRET between the ribosome (MDCC at position 21 of protein uL23) and SecYEG (Alexa 488 at position 111 of SecY) (Supporting Information Fig. S4). The addition of FtsY or FtsY-A207 reduces the amplitude of the donor fluorescence change at saturation to various extents (Fig. 7). The observed fluorescence changes are not due to binding competition, as the quantitative evaluation of the titration curves (see “Experimental Procedures” section) reveals that there is no increase of the apparent K_d over the whole range of FtsY construct concentrations, which indicates that FtsY binding to SecYEG in complex with ribosomes is non-competitive. However, in the ternary complex the arrangement of SecYEG relative to the ribosome is changed, as suggested by the observed differences in FRET efficiencies. The observation that FtsY-A207 has a similar effect as full-length FtsY, while the effects with the other domains are smaller or absent, is consistent with a major role of the A domain and the MTS in complex formation with SecYEG.

Discussion

Previous work has shown that the formation of a ternary targeting complex, that is recruitment of SRP to RNCs and, subsequently, enhanced SRP binding to FtsY, is

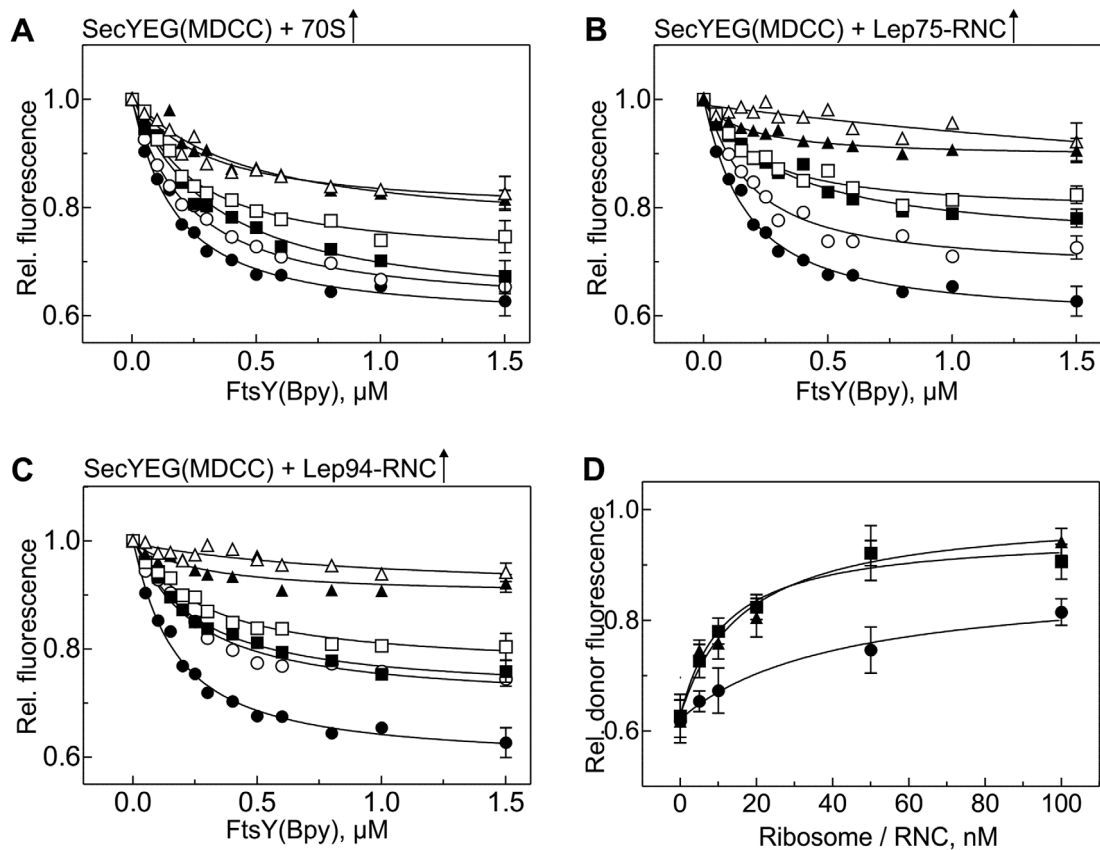


Fig. 6. Concurrent binding of FtsY and ribosomes to SecYEG.

A–C. SecYEG(MDCC) (50 nM) was titrated with FtsY(Bpy) in the presence of increasing concentrations (\uparrow) of (A) vacant 70S ribosomes, (B) Lep75-RNCs, or (C) Lep94-RNCs, monitoring the decrease of donor fluorescence due to FRET. 70S/RNC concentrations (nM): none (\bullet), 5 (\circ), 10 (\blacksquare), 20 (\square), 50 (\blacktriangle), 100 (\triangle). Apparent K_d values of FtsY(Bpy) binding to SecYEG(MDCC) were determined by nonlinear fitting (see “Experimental Procedures” section) and remained constant at $K_d = 0.2 \pm 0.1 \mu\text{M}$ up to the highest ribosome/RNC concentration.

D. The donor fluorescence at saturating FtsY(Bpy) concentrations from panels (A) to (C) is plotted against the concentration of added vacant ribosomes (\bullet), Lep75-RNCs (\blacksquare), or Lep94-RNCs (\blacktriangle). The data were evaluated by fitting (see “Experimental Procedures” section), yielding apparent K_d values of the complexes of SecYEG with vacant ribosomes (20 ± 10 nM), Lep75-RNCs (8 ± 2 nM), or Lep94-RNCs (16 ± 2 nM), in the presence of FtsY; error margins are SEM ($n = 2$).

promoted by the interaction of SRP with RNCs having the peptide exit tunnel filled or exposing an SAS (Bornemann *et al.*, 2008; Saraogi *et al.*, 2014). The effect results from the stabilization of the RNC–SRP complex during the phase in which SRP scans ribosomes (Holtkamp *et al.*, 2012). FtsY binding to RNC-bound SRP is enhanced by an induced conformational change of SRP exposing the NG domain of SRP for binding to the NG domain of FtsY (Bornemann *et al.*, 2008; Buskiewicz *et al.*, 2009). Accordingly, current models of membrane targeting (Holtkamp *et al.*, 2012; Saraogi *et al.*, 2014; Jomaa *et al.*, 2016) include a conformational change of SRP that is induced by interactions with both the ribosome and the nascent chain and promotes complex formation with FtsY. The present work shows that targeting complex formation is further enhanced substantially when FtsY is presented in a complex with SecYEG embedded in membrane phospholipids, rather than free

in solution. In keeping with the observation that non-membrane-bound FtsY is impaired in targeting complex formation (Valent *et al.*, 1998; Mircheva *et al.*, 2009), binding to the translocon activates FtsY for complex formation with ribosome-bound SRP.

According to *in-vivo* data, FtsY in the cell is mainly located at the membrane, interacting with both lipids and the translocon (Mircheva *et al.*, 2009; Braig *et al.*, 2009; Kuhn *et al.*, 2011, 2015). The present *in-vitro* analysis is consistent with this and suggests that the A and NG domains of FtsY contribute about equally to this interaction, in that the isolated domains bind to lipid-embedded SecYEG with $K_d = 0.2 \mu\text{M}$ each. The interactions of the NG and the A domains with SecYEG appear to be independent of one another. The binding of FtsY to the translocon entails protein-protein interactions and, to a lesser extent, protein-lipid interactions, as suggested by K_d values of 1.2 and $0.2 \mu\text{M}$ for FtsY binding

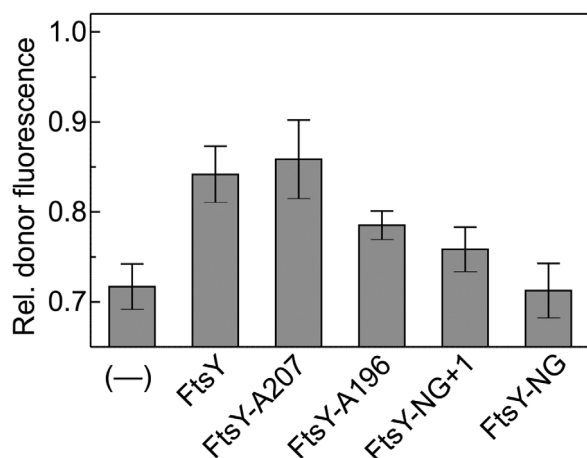


Fig. 7. Rearrangement of the SecYEG–ribosome complex on concurrent binding of FtsY or FtsY domains. Vacant 70S ribosomes labelled with MDCC (donor) (5 nM) were titrated with SecYEG(Alx488) (acceptor) in the presence of increasing concentrations (up to 10 μ M) of FtsY or FtsY domains (Supporting Information Fig. S4). Final levels of donor fluorescence at saturation, relative to the initial donor fluorescence measured prior to the addition of SecYEG(Alx488), are plotted (grey columns); error margins are SD ($n = 3\text{--}4$). Apparent K_d values of SecYEG binding to ribosomes, as determined by fitting the titration curves (Supporting Information Fig. S4), were $0.2 \pm 0.1 \mu\text{M}$, independent of added FtsY or FtsY domain.

to empty nanodiscs and SecYEG-containing nanodiscs respectively (Kuhn *et al.*, 2015). Nevertheless, the presence of phospholipids is essential for FtsY binding to SecYEG, as complex formation is not observed when SecYEG is solubilized by adding a detergent (Kuhn *et al.*, 2015). This behaviour may be related to observations that anionic phospholipids, which are enriched in the lipid shell of SecYEG (Prabudiansyah *et al.*, 2015), as also observed for our SecYEG-containing nanodiscs (see “Experimental Procedures” section), prime FtsY for its function in binding to SRP and subsequent steps in the targeting pathway (Lam *et al.*, 2010; Stjepanovic *et al.*, 2011).

Crosslinking data indicate that the interaction between FtsY and SecYEG is mainly mediated by the A domain and to a lesser extent by the NG domain of FtsY (Kuhn *et al.*, 2011). Accordingly, our data show that the A domain has a significant contribution to the binding of FtsY to the SecYEG–RNC complex, whereas FtsY-NG/NG + 1, which lack the A domain, hardly participate in ternary complex formation. The observed reduction in FRET between the ribosome and SecYEG in the presence of A domain constructs indicates a rearrangement of the complex which is induced by the A domain and appears to be dependent on both lipid-binding sequences of FtsY.

As we show here, unbound FtsY is present in a conformation in which the NG and A domains are engaged

in interactions with one another that impair the interaction of FtsY with SRP, the central element of targeting complex formation. According to the NMR spectra, the interaction with the NG domain appears to be restricted to residues near the C terminus of the FtsY-A207 construct, including residues 185–197 of the MTS. The formation of a few hydrogen bonds or electrostatic interactions would be consistent with the observed affinity of the complex of the two domains ($K_d = 10 \text{ nM}$). The domains appear to interact in full-length FtsY as well, as suggested by NMR and the formation of short-distance crosslinks between A and G domains. FtsY with cross-linked A and G domains is impaired in binding to SRP, indicating that FtsY, to promote its function as an SRP receptor, has to rearrange into a conformation in which NG and A domains are separated. The energy to be used for the separation of the domains would explain why full-length FtsY binds to SecYEG with the same affinity as either domain alone. In fact, the present data show that binding to SecYEG induces a rearrangement of FtsY into an open form which binds to SRP with enhanced affinity, whereas binding to *E. coli* membrane phospholipids in nanodiscs alone, without SecYEG, does not. This observation is in keeping with a previous report where *E. coli* phospholipids in liposomes did not enhance FtsY–SRP complex formation, in contrast to liposomes containing a much higher proportion of anionic phospholipids (Lam *et al.*, 2010). The rearrangement accompanying complex formation is probably related to a previously reported conformational switch of the MTS region triggered by anionic phospholipid binding (Stjepanovic *et al.*, 2011).

A central element of the present model of targeting complex formation is that unbound FtsY is present in a conformation that is ineffective in binding to SRP and needs to be activated by binding to the translocon. The activating rearrangement probably involves the transfer of a region of FtsY comprising the MTS from the NG domain to SecYEG, presumably the C5 loop (Kuhn *et al.*, 2015), which renders the NG domain accessible for the interaction with the NG domain of SRP protein Ffh. The rearrangement may be related to a rearrangement of the N1 helix of FtsY that accompanies FtsY binding to SRP/Ffh (Neher *et al.*, 2008). Activation of FtsY by complex formation with the translocon, perhaps supported by anionic phospholipids surrounding the translocon, provides a means to adjust both localization and amount of activated FtsY to the available translocons in the cell. That way it can be avoided, or at least minimized, that unbound FtsY, which is present at high concentration in the cell (17 μM) (Kudva *et al.*, 2013), sequesters SRP, which is present at 50-fold lower concentration, and thereby interferes with effective targeting of RNCs by SRP.

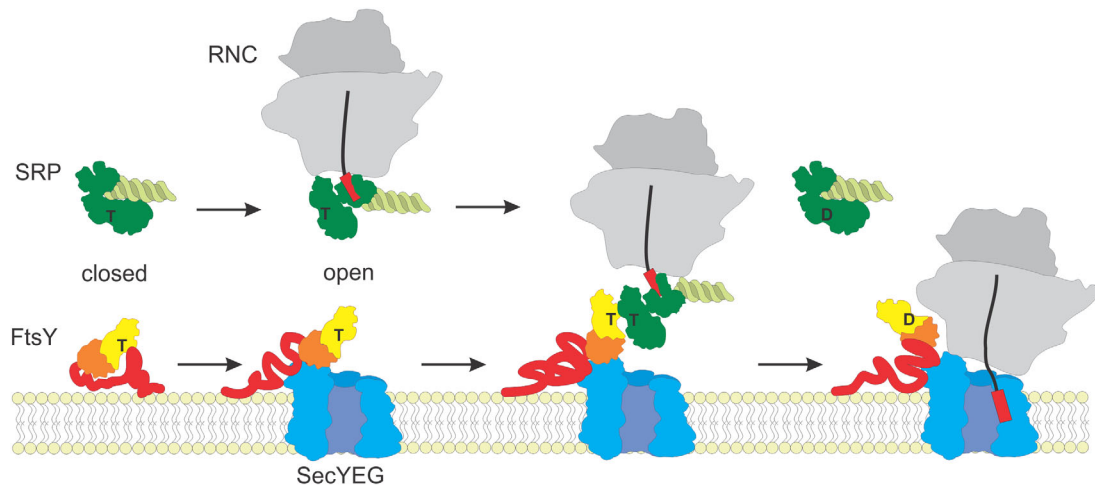


Fig. 8. Model of quaternary targeting complex formation. Free FtsY is present in a closed conformation in which the NG domain (yellow-orange) and the A domain (red; arbitrary shape) interact. Binding of FtsY to SecYEG induces a domain rearrangement, activating FtsY for the interaction with SRP by exposing the NG domain. Unbound SRP consisting of Ffh protein (dark green) and 4.5S RNA (light green) initially is present in a closed conformation as well. Binding to an RNC (not drawn to scale) exposing a signal-anchor sequence (red rectangle) induces opening of SRP. Thereby the NG domain is exposed (Buskiewicz *et al.*, 2009), promoting the SRP–FtsY interaction (Holtkamp *et al.*, 2012) and the formation of the quaternary targeting complex. Following nascent-chain transfer the targeting complex is disassembled, induced by GTP hydrolysis by both Ffh and FtsY. FtsY can remain bound to the SecYEG–RNC complex, whereas SRP is released to enter another round of targeting. Guanine nucleotides bound to the G domains of Ffh and FtsY are indicated by T (GTP) or D (GDP).

The interaction of FtsY with phospholipid-embedded SecYEG that induces the formation of an active open conformation of FtsY is an important element regulating a key event in membrane targeting, that is the interaction of SRP and FtsY (Fig. 8). The regulation appears to happen in an analogous way for FtsY and SRP, as SRP binding to RNCs exposing an SAS strongly promotes the SRP–FtsY interaction (Bornemann *et al.*, 2008) by enhancing the accessibility of the Ffh–NG domain (Buskiewicz *et al.*, 2009). Taken together, these results suggest that direct RNC transfer to the translocon is guided by the interaction between RNC-bound SRP and translocon-bound FtsY in a quaternary transfer complex (Fig. 8). Thus, translocon-bound FtsY has a central role in targeting ribosomes to the membrane. Following RNC transfer to the translocon and during continued peptide elongation FtsY can remain bound to the translocon. This may be of importance for the translocon–FtsY complex to rapidly enter a new round of targeting after the completion of the synthesis of one membrane protein.

Experimental procedures

FtsY constructs

FtsY was cloned from the pET9a vector coding for C-terminally His-tagged FtsY to a pET-SUMO vector (Invitrogen) coding for FtsY with N-terminal His₆-tag and a SUMO cleavage site between the first Met and the tag, using the In-fusion cloning strategy (ClonTech). The vector was amplified using primers 5'-GATCCGGCTGCTAACAAAGCC

CGAAAG-3' and 3'-ACCACCAATCTGTTCTCTGTGAGCCT CAATAATATC-5'. FtsY was amplified using primers 5'-GAA CAGATTGGTGGTATGGCGAAAGAAAAAACG-3' and 3'-GTTAGCAGCCGGATCTTAATCCTCTCGGGC-5' (underlined are the sequences that overlap between vector and insert). The FtsY mutants F196stop, K207stop, A167C, F196C and V342C, G357C, L407C, S422C, G439C, T451C, as well as mutant SecY(S111C) were generated by site-directed mutagenesis using Phusion polymerase (New England Biolabs).

Expression and purification of FtsY and ffh

FtsY was expressed from the pET9a vector and FtsY-A196/207 were expressed from pET-SUMO vectors with N-terminal His₆-tags; the FtsY-NG and FtsY-NG + 1 domains were expressed from pT7-5(NG) and pT7-5(NG + 1) vectors with C-terminal His₆-tags (Parlitz *et al.*, 2007) (a gift from Eitan Bibi, Weizman Institute of Science, Rehovot, Israel). All FtsY variants were expressed in *E. coli* BL21(DE3)pLysS and purified following a published protocol (Buskiewicz *et al.*, 2005). Cells were opened in an Emulsi-Flex C3 homogenizer (Avestin) in buffer B (20 mM HEPES, pH 7.5, 150 mM KCl, 20 mM imidazole, 10% (w/v) glycerol) supplemented with 0.01% (v/v) nona-ethylene glycol monododecyl ether (Nikkol) and cComplete EDTA-free protease inhibitor (Roche). The lysate was then cleared by centrifugation at 45,000g for 45 min and applied on a nickel-affinity column. The column was washed with buffer B containing 1 M KCl, followed by buffer B without added KCl, and finally the protein was eluted with buffer B containing 0.2 M imidazole. Buffer exchange in the fractions containing FtsY, FtsY-A196, or FtsY-A207 into buffer C (20 mM HEPES pH 7.5, 150 mM KCl, 10% glycerol, 1 mM dithiothreitol (DTT))

was carried out using a PD-10 desalting column (GE Healthcare). Proteins were further purified by chromatography on a HiTrap Q HP anion exchange column (GE Healthcare), and eluted by applying a gradient of 0.15–0.5 M KCl in buffer C. The His₆-tags of FtsY-A196 and FtsY-A207 were cleaved by incubation with His₆-tagged Ulp1 protease (1:100 protease:protein ratio) for 15 hours at 4°C; protease and His-tag were removed by nickel-affinity chromatography. FtsY-NG and FtsY-NG + 1 constructs were further purified on HiTrap SP HP cation exchange column (GE Healthcare) in buffer D (20 mM HEPES, pH 7.5, 60 mM NH₄Cl, 50 mM KCl, 7 mM MgCl₂, 10% glycerol, 1 mM DTT) and eluted in a gradient from 0.05–1 M KCl in buffer D. Purified proteins were dialyzed against buffer A and stored at –80°C.

Ffh with an N-terminal His₆-tag was expressed from a pET24 vector in *E. coli* BL21(DE3)pLysS and purified according to a published protocol (Buskiewicz *et al.*, 2005) with some modifications. Cells were opened as above in buffer E (20 mM HEPES, pH 7.5, 60 mM NH₄Cl, 150 mM KCl, 7 mM MgCl₂, 20 mM imidazole) supplemented with cOmplete EDTA-free protease inhibitor. Cell debris was removed by centrifugation (45 min at 20,000g, JA 25.50 rotor, Beckman Coulter) and the supernatant was loaded on a nickel-affinity column. Ffh was eluted in buffer E containing 0.5 M KCl and 0.25 M imidazole. Ffh was purified further by cation exchange chromatography following the same protocol as used for the purification of the FtsY-NG/NG + 1 constructs (see above). The purified protein was stored in buffer A.

Expression and purification of SecYEG and MSP1D1

SecYEG and SecY(S111C)EG containing N-terminally His₆-tagged SecE were prepared by a published protocol (Ge *et al.*, 2014). SecYEG was expressed in *E. coli* strain Lemo21(DE3) (New England Biolabs); expression was induced at OD₆₀₀ = 0.6 by adding 0.4 mM IPTG, and cell growth was continued for 4 hours at 37°C. Cells were opened in an Emulsiflex C3 homogenizer (Avestin) in buffer F (20 mM Tris-HCl, pH 7.5, 200 mM NaCl, 5 mM MgCl₂, 10% glycerol), supplemented with cOmplete EDTA-free protease inhibitor (Roche). The lysate was cleared for 20 min at 30,000g (JA 25.50 rotor, Beckman Coulter), and cell membranes were isolated by ultracentrifugation (120 min at 150,000g, Ti 50.2 rotor, Beckman Coulter). Protein was solubilized by incubating the pellets for 1 hour at 4°C in buffer G (20 mM Tris-HCl, pH 7.5, 1 M NaCl, 5 mM MgCl₂, 5 mM imidazole, 1% (w/v) n-dodecyl-β-D-maltoside (DDM), 10% glycerol) and the suspension was clarified by ultracentrifugation (25 min, 75,000g). Protein in the supernatant was subjected to nickel-affinity chromatography (Ni-IDA, Macherey-Nagel), as follows. After loading, the column was washed with buffer F supplemented with 10 mM imidazole and 0.03% DDM; protein was eluted in buffer F supplemented with 0.2 M imidazole and 0.03% DDM. Fractions containing SecYEG were collected and rebuffed in buffer H (50 mM HEPES, pH 8.0, 50 mM NaCl, 10% glycerol, 0.03% DDM, 1 mM DTT) and applied on a HiTrap SP HP cation exchange column (5 ml; GE Healthcare). SecYEG

was eluted by applying a 40 ml gradient from 0.05 to 0.6 M NaCl in buffer H. Fractions containing protein were collected, concentrated and stored in buffer A supplemented with 0.03% DDM.

The membrane-scaffold protein, MSP1D1, was expressed from plasmid 20061 (Addgene) in *E. coli* BL21(DE3). Cells were opened as above in buffer I (20 mM Tris-HCl, pH 8.0, 1% Triton-X, 0.01% Nikkol) supplemented with cOmplete EDTA-free protease inhibitor; the lysate was cleared by centrifugation for 30 min at 75,000g (rotor JA 30.50, Beckman Coulter). The supernatant was applied onto a nickel-affinity column, as above; material bound unspecifically was eluted with buffer J (10 mM Tris-HCl, pH 8.0, 0.5 M NaCl, 10% glycerol) supplemented with 1% Triton X-100, then with buffer J supplemented with 50 mM sodium cholate, followed by buffer J supplemented with 5 mM imidazole; finally the protein was eluted with 0.2 M imidazole in buffer J. Fractions containing the MSP1D1 protein were collected and dialyzed against buffer A (Bayburt and Sligar, 2010; Ge *et al.*, 2014).

Fluorescence labelling of proteins

Protein labelling at cysteine residues by maleimide chemistry was performed following the protocol provided by the manufacturer (Invitrogen) using buffer C (supplemented with 0.03% DDM for SecYEG labelling) and incubating the protein with a fivefold excess of dye for 2 hours at room temperature. Unreacted dye was removed on a PD-10 desalting column and labelled proteins were stored in buffer A. Labelling efficiencies were >90%, based on absorbance measurements.

Incorporation of SecYEG into nanodiscs

SecYEG reconstitution into nanodiscs and the assembly of empty nanodiscs were performed following a published procedure (Ge *et al.*, 2014). For the assembly of SecYEG-containing nanodiscs, the mixture of SecYEG, the membrane-scaffold protein MSP1D1, and *E. coli* total lipids (Avanti Polar Lipids), containing about 73% phosphatidylethanolamine (PE), 24% phosphatidylglycerol (PG), and a small amount (< 4%) of cardiolipin (CL), was incubated for 1 hour on ice in buffer A containing 0.1% DDM. Subsequently, nanodisc assembly was initiated by the addition of BioBeads SM-2 (BIO-RAD) and gentle agitation at 4°C overnight. SecYEG-containing nanodiscs were purified by size-exclusion chromatography (Superdex 200 PG 16/100; GE Healthcare). These SecYEG-containing nanodiscs, which were used for all experiments with SecYEG, were enriched in PG (about 70%), according to the analysis by ¹H-NMR (see below). Empty nanodiscs were prepared in the same way, except that SecYEG was omitted. The phospholipid composition of empty nanodiscs (ND) was PE (about 62%), PG (about 37%), and cardiolipin (< 2%), as in the input mixture. For better comparison with SecYEG-containing nanodiscs, empty nanodiscs with a higher content of PG (ND*) were prepared in the same way, using 25% PE, 70% PG and 5% CL.

For lipid analysis by NMR the aqueous samples were lyophilized overnight, followed by addition of chloroform:methanol:water (2:1:1); the chloroform layer was separated, washed with half a volume of water and an equal volume of

0.5 M NaCl, concentrated on a rotary evaporator, dried and redissolved in MeOH-*d*₄:CHCl₃-*d*₁ 1:1. ¹H-NMR spectra were recorded at 283 K on a 400 MHz Bruker Avance spectrometer (Bruker, Rheinstetten, Germany) equipped with a TXI HCN z-gradient probe. Spectra were processed using TOPSPIN2 (Bruker, Karlsruhe, Germany). Spectra were assigned by chemical shift analysis and comparison with standards (PE, PG, CL) (Avanti Polar Lipids).

RNC preparation

Ribosomes from *E. coli* MRE600, initiation factors IF1, IF2, and IF3, EF-Tu, EF-G, f[³H]Met-tRNA^{Met} and total aminoacyl-tRNA were prepared as described (Rodnina and Wintermeyer, 1995). Ribosomes labelled with MDCC at position S21C of ribosomal protein uL23 were prepared as previously described (Holtkamp *et al.*, 2012). RNCs with wild-type or MDCC-labelled ribosomes were prepared by *in-vitro* translation of truncated mRNAs coding for the N-terminal 75 or 94 amino acids of leader peptidase (Lep75- or Lep94-RNC) (Bornemann *et al.*, 2008). In a typical RNC preparation, about 80% of the ribosomes carried a peptide chain of the indicated length.

Fluorescence titrations and data evaluation

Fluorescence titrations were performed on a Fluorolog-3 fluorimeter (Horiba) at 25°C in buffer A (20 mM HEPES, pH 7.5, 70 mM NH₄Cl, 30 mM KCl, 7 mM MgCl₂, 10% glycerol) at 25°C in the presence of 0.5 mM GDPNP, unless indicated otherwise. MDCC emission was measured at 460 nm upon excitation at 430 nm. Bpy was excited at 480 nm and the emission was measured at 520 nm. For fluorescence anisotropy measurements, standard software (FluorEssence v3.5) settings were used. Titration curves were evaluated in terms of *K_d* using a quadratic equation (Kuhn *et al.*, 2015). To estimate the apparent *K_d* for the binding of Lep75/94-RNC or vacant ribosomes to SecYEG in the presence of FtsY, the dependence of the final relative donor (MDCC) signal was analyzed at increasing ribosome concentration (Kuhn *et al.*, 2015).

GTPase assay

GTP hydrolysis was measured at multiple-turnover conditions, that is at an excess of GTP (100 μM) over FtsY or FtsY-NG (5 μM). Experiments were performed in triplicate at 25°C in buffer A. Reactions were initiated by the addition of GTP doped with [γ-³²P]GTP. The initial velocity was measured by taking aliquots at specific time points, and the reaction was stopped by adding 50% formic acid (Rodnina *et al.*, 1999). Products were separated by thin layer chromatography on PEI 300 Polygram plates (Macherey-Nagel) with 0.5 M KH₂PO₄, pH 3.5, as mobile phase. Radioactive spots were visualized on a FLA-7000 biomolecular imager (GE Healthcare) and quantified using densitometry software (MultiGauge, Fujifilm). The relative amount of hydrolyzed GTP was calculated from the ratio of ³²P-labelled inorganic

phosphate formed by GTP hydrolysis relative to total radioactivity per lane.

Dibromobimane crosslinking

The bifunctional crosslinker dibromobimane (dB) was used to crosslink cysteine residues at positions 167 in the A domain of FtsY and various positions in the NG domain. dB has two equivalent bromomethyl groups that can crosslink two thiol groups within 3–6 Å distance (Mornet *et al.*, 1985). Double-cysteine mutants of FtsY (1 μM) were treated with a fivefold excess of dB for 2 hours at 25°C in buffer A. Crosslinked products were resolved on 12% Tris-glycine sodium dodecyl sulfate polyacrylamide gel electrophoresis (SDS-PAGE). As a control, double-cysteine FtsY variants were treated with monobromobimane (mB). Proteins were visualized by Coomassie staining.

Gel shift assay

SRP-FtsY complex formation was monitored by 7% non-denaturing polyacrylamide gel electrophoresis as described previously (Jagath *et al.*, 2000) with the following modifications. Complexes were prepared by incubating 4.5S RNA (2 μM), Ffh (2 μM), and FtsY or mB- or dB-treated FtsY (2 μM) in buffer A in the presence of 0.5 mM GDPNP at 25°C for 5 min. RNA was visualized by staining with GelRed (Biotium).

Nascent peptide protection by SecYEG

To compare the functionality of SecYEG labelled at position S111C of SecY with non-labelled SecYEG we have monitored the protection against proteinase K digestion of the N-terminal SAS of Lep75-RNC, using an established protocol (Ge *et al.*, 2014). Lep75-RNC (0.2 μM) labelled with Bpy at the N-terminal methionine was incubated with SecYEG in nanodiscs (2 μM) and proteinase K (1.5 mg/ml) at 37°C. Samples were quenched with phenylmethylsulfonyl fluoride (45 mM). The nascent peptide was set free by RNaseA digestion (10 mg/ml; 30 min, 37°C). Samples (0.5 pmol) were analyzed by Tris-Tricine denaturing polyacrylamide gel electrophoresis; N-terminal peptides were visualized by the fluorescence of Bpy.

NMR measurements

¹⁵N¹H TROSY-HSQC spectra of ²H¹⁵N¹³C-enriched full-length FtsY (132 μM) and ²H¹⁵N¹³C-enriched FtsY-A207 (135.4 μM) in buffer C (20 mM HEPES, pH 7.5, 150 mM KCl, 10% glycerol, 1 mM dithiothreitol) were recorded at 700 MHz and 5°C on a Bruker Avance I NMR spectrometer equipped with a TXI cryogenic probe.

To study interactions between the A and NG domains of FtsY, unlabelled FtsY-NG domain (32 μM) and ²H¹⁵N¹³C-labelled FtsY-A207 (31 μM) were measured in buffer C containing 20 μl D₂O. ¹⁵N¹H TROSY-HSQC spectra were recorded at 600 MHz and 5°C with a total experimental time of 5.5 hours per spectrum. Resonance intensities were

compared with a reference spectrum where an equal volume of buffer was added instead of the NG domain. Resonances were assigned to individual amino acids as described elsewhere (Lakomek *et al.*, 2016).

Author contributions

W.W., N.L., A.D. and T.B. designed experiments, A.D. prepared materials, carried out experiments and analyzed data, N.L. performed the 2D NMR measurements and data analysis, S.R. performed lipid analyses by NMR, W.W., A.D. and N.L. wrote the article.

Acknowledgements

We thank Eitan Bibi for FtsY constructs, Marina Rodnina and Evan Mercier for valuable suggestions on the manuscript, Anna Pfeifer and Franziska Hummel for expert technical assistance, and Johannes Jöckel for help in the initial phase of the project. The work was supported by the DFG/NIH Research Career Transition award program (to N.L., grant number DFG LA 2724/1-1). The authors declare no competing financial interest.

References

- Akopian, D., Dalal, K., Shen, K., Duong, F., and Shan, S.O. (2013) SecYEG activates GTPases to drive the completion of cotranslational protein targeting. *J Cell Biol* **200**: 397–405.
- Alami, M., Dalal, K., Lelj-Garolla, B., Sligar, S.G., and Duong, F. (2007) Nanodiscs unravel the interaction between the SecYEG channel and its cytosolic partner *seca*. *EMBO J* **26**: 1995–2004.
- Angelini, S., Deitermann, S., and Koch, H.G. (2005) FtsY, the bacterial signal-recognition particle receptor, interacts functionally and physically with the SecYEG translocon. *EMBO Rep* **6**: 476–481.
- Angelini, S., Boy, D., Schiltz, E., and Koch, H.G. (2006) Membrane binding of the bacterial signal recognition particle receptor involves two distinct binding sites. *J Cell Biol* **174**: 715–724.
- Bahari, L., Parlitz, R., Eitan, A., Stjepanovic, G., Bochkareva, E.S., Sinning, I., and Bibi, E. (2007) Membrane targeting of ribosomes and their release require distinct and separable functions of FtsY. *J Biol Chem* **282**: 32168–32175.
- Bayburt, T.H., and Sligar, S.G. (2010) Membrane protein assembly into Nanodiscs. *FEBS Lett* **584**: 1721–1727.
- Bernstein, H.D., Poritz, M.A., Strub, K., Hoben, P.J., Brenner, S., and Walter, P. (1989) Model for signal sequence recognition from amino-acid sequence of 54K subunit of signal recognition particle. *Nature* **340**: 482–486.
- Bernstein, H.D., Zopf, D., Freymann, D.M., and Walter, P. (1993) Functional substitution of the signal recognition particle 54-kDa subunit by its *escherichia coli* homolog. *Proc Natl Acad Sci USA* **90**: 5229–5233.
- Bibi, E., Herskovits, A.A., Bochkareva, E.S., and Zelazny, A. (2001) Putative integral membrane SRP receptors. *Trends Biochem Sci* **26**: 15–16.
- Bornemann, T., Joeckel, J., Rodnina, M.V., and Wintermeyer, W. (2008) Signal sequence-independent membrane targeting of ribosomes containing short nascent peptides within the exit tunnel. *Nat Struct Mol Biol* **15**: 494–499.
- Braig, D., Bar, C., Thumfart, J.O., and Koch, H.G. (2009) Two cooperating helices constitute the lipid-binding domain of the bacterial SRP receptor. *J Mol Biol* **390**: 401–413.
- Burk, J., Weiche, B., Wenk, M., Boy, D., Nestel, S., Heimrich, B., and Koch, H.G. (2009) Depletion of the signal recognition particle receptor inactivates ribosomes in *escherichia coli*. *J Bacteriol* **191**: 7017–7026.
- Buskiewicz, I., Kubarenko, A., Peske, F., Rodnina, M.V., and Wintermeyer, W. (2005) Domain rearrangement of SRP protein ffh upon binding 4.5S RNA and the SRP receptor FtsY. *RNA* **11**: 947–957.
- Buskiewicz, I.A., Jockel, J., Rodnina, M.V., and Wintermeyer, W. (2009) Conformation of the signal recognition particle in ribosomal targeting complexes. *RNA* **15**: 44–54.
- de Leeuw, E., Poland, D., Mol, O., Sinning, I., ten Hagen-Jongman, C.M., Oudega, B., and Luirink, J. (1997) Membrane association of FtsY, the *E. Coli* SRP receptor. *FEBS Lett* **416**: 225–229.
- de Leeuw, E., Te Kaat, K., Moser, C., Menestrina, G., Demel, R., de Kruijff, B., *et al.* (2000) Anionic phospholipids are involved in membrane association of FtsY and stimulate its GTPase activity. *EMBO J* **19**: 531–541.
- Denisov, I.G., Grinkova, Y.V., Lazarides, A.A., and Sligar, S.G. (2004) Directed self-assembly of monodisperse phospholipid bilayer nanodiscs with controlled size. *J Am Chem Soc* **126**: 3477–3487.
- Egea, P.F., Shan, S.O., Napetschnig, J., Savage, D.F., Walter, P., and Stroud, R.M. (2004) Substrate twinning activates the signal recognition particle and its receptor. *Nature* **427**: 215–221.
- Eitan, A., and Bibi, E. (2004) The core *escherichia coli* signal recognition particle receptor contains only the N and G domains of FtsY. *J Bacteriol* **186**: 2492–2494.
- Focia, P.J., Shepotinovskaya, I.V., Seidler, J.A., and Freymann, D.M. (2004) Heterodimeric GTPase core of the SRP targeting complex. *Science* **303**: 373–377.
- Frauenfeld, J., Gumbart, J., Sluis, E.O., Funes, S., Gartmann, M., Beatrix, B., *et al.* (2011) Cryo-EM structure of the ribosome-SecYE complex in the membrane environment. *Nat Struct Mol Biol* **18**: 614–621.
- Ge, Y., Draycheva, A., Bornemann, T., Rodnina, M.V., and Wintermeyer, W. (2014) Lateral opening of the bacterial translocon on ribosome binding and signal peptide insertion. *Nat Commun* **5**: 5263.
- Haddad, A., Rose, R.W., and Pohlschroder, M. (2005) The haloferax volcanii FtsY homolog is critical for haloarchaeal growth but does not require the a domain. *J Bacteriol* **187**: 4015–4022.
- Halic, M., Blau, M., Becker, T., Mielke, T., Pool, M.R., Wild, K., Sinning, I., and Beckmann, R. (2006) Following the signal sequence from ribosomal tunnel exit to signal recognition particle. *Nature* **444**: 507–511.

- Holtkamp, W., Lee, S., Bornemann, T., Senyushkina, T., Rodnina, M.V., and Wintermeyer, W. (2012) Dynamic switch of the signal recognition particle from scanning to targeting. *Nat Struct Mol Biol* **19**: 1332–1337.
- Jagath, J.R., Rodnina, M.V., and Wintermeyer, W. (2000) Conformational changes in the bacterial SRP receptor FtsY upon binding of guanine nucleotides and SRP. *J Mol Biol* **295**: 745–753.
- Jomaa, A., Boehringer, D., Leibundgut, M., and Ban, N. (2016) Structures of the E. Coli translating ribosome with SRP and its receptor and with the translocon. *Nat Commun* **7**: 10471.
- Kedrov, A., Kusters, I., and Driessen, A.J. (2013) Single-molecule studies of bacterial protein translocation. *Biochemistry* **52**: 6740–6754.
- Kudva, R., Denks, K., Kuhn, P., Vogt, A., Muller, M., and Koch, H.G. (2013) Protein translocation across the inner membrane of Gram-negative bacteria: The sec and tat dependent protein transport pathways. *Res Microbiol* **164**: 505–534.
- Kuhn, P., Weiche, B., Sturm, L., Sommer, E., Drepper, F., Warscheid, B., Sourjik, V., and Koch, H.G. (2011) The bacterial SRP receptor, SecA and the ribosome use overlapping binding sites on the SecY translocon. *Traffic* **12**: 563–578.
- Kuhn, P., Draycheva, A., Vogt, A., Petriman, N.A., Sturm, L., Drepper, F., et al. (2015) Ribosome binding induces repositioning of the signal recognition particle receptor on the translocon. *J Cell Biol* **211**: 91–104.
- Kusters, R., Lentzen, G., Eppens, E., van Geel, A., van der Weijden, C.C., Wintermeyer, W., and Luirink, J. (1995) The functioning of the SRP receptor FtsY in protein-targeting in E. Coli is correlated with its ability to bind and hydrolyse GTP. *FEBS Lett* **372**: 253–258.
- Lakomek, N.A., Draycheva, A., Bornemann, T., and Wintermeyer, W. (2016) Electrostatics and intrinsic disorder drive translocon binding of the SRP receptor FtsY. *Angew Chem Int Ed*, DOI:10.1002/anie.201602905.
- Lam, V.Q., Akopian, D., Rome, M., Henningsen, D., and Shan, S.O. (2010) Lipid activation of the signal recognition particle receptor provides spatial coordination of protein targeting. *J Cell Biol* **190**: 623–635.
- Luirink, J., ten Hagen-Jongman, C.M., van der Weijden, C.C., Oudega, B., High, S., Dobberstein, B., and Kusters, R. (1994) An alternative protein targeting pathway in escherichia coli: Studies on the role of FtsY. *EMBO J* **13**: 2289–2296.
- Mircheva, M., Boy, D., Weiche, B., Hucke, F., Graumann, P., and Koch, H.G. (2009) Predominant membrane localization is an essential feature of the bacterial signal recognition particle receptor. *BMC Biol* **7**: 76.
- Mornet, D., Ue, K., and Morales, M.F. (1985) Stabilization of a primary loop in myosin subfragment 1 with a fluorescent crosslinker. *Proc Natl Acad Sci USA* **82**: 1658–1662.
- Neher, S.B., Bradshaw, N., Floor, S.N., Gross, J.D., and Walter, P. (2008) SRP RNA controls a conformational switch regulating the SRP-SRP receptor interaction. *Nat Struct Mol Biol* **15**: 916–923.
- Neumann-Haefelin, C., Schafer, U., Muller, M., and Koch, H.G. (2000) SRP-dependent co-translational targeting and SecA-dependent translocation analyzed as individual steps in the export of a bacterial protein. *EMBO J* **19**: 6419–6426.
- Park, E., and Rapoport, T.A. (2012) Mechanisms of Sec61/SecY-mediated protein translocation across membranes. *Annu Rev Biophys* **41**: 21–40.
- Park, E., Menetret, J.F., Gumbart, J.C., Ludtke, S.J., Li, W., Whynot, A., Rapoport, T.A., and Akey, C.W. (2014) Structure of the SecY channel during initiation of protein translocation. *Nature* **506**: 102–106.
- Parlitz, R., Eitan, A., Stjepanovic, G., Bahari, L., Bange, G., Bibi, E., and Sinning, I. (2007) Escherichia coli signal recognition particle receptor FtsY contains an essential and autonomous membrane-binding amphipathic helix. *J Biol Chem* **282**: 32176–32184.
- Peluso, P., Herschlag, D., Nock, S., Freymann, D.M., Johnson, A.E., and Walter, P. (2000) Role of 4.5S RNA in assembly of the bacterial signal recognition particle with its receptor. *Science* **288**: 1640–1643.
- Peluso, P., Shan, S.O., Nock, S., Herschlag, D., and Walter, P. (2001) Role of SRP RNA in the GTPase cycles of ffh and FtsY. *Biochemistry* **40**: 15224–15233.
- Powers, T., and Walter, P. (1997) Co-translational protein targeting catalyzed by the Escherichia coli signal recognition particle and its receptor. *EMBO J* **16**: 4880–4886.
- Prabudiansyah, I., Kusters, I., Caforio, A., and Driessen, A.J. (2015) Characterization of the annular lipid shell of the sec translocon. *Biochim Biophys Acta* **1848**: 2050–2056.
- Reinau, M.E., Thogersen, I.B., Enghild, J.J., Nielsen, K.L., and Otzen, D.E. (2010) The diversity of FtsY-lipid interactions. *Biopolymers* **93**: 595–606.
- Rodnina, M.V., and Wintermeyer, W. (1995) GTP consumption of elongation factor tu during translation of heteropolymeric mRNAs. *Proc Natl Acad Sci U S A* **92**: 1945–1949.
- Rodnina, M.V., Savelsbergh, A., Matassova, N.B., Katunin, V.I., Semenov, Y.P., and Wintermeyer, W. (1999) Thio-strepton inhibits the turnover but not the GTPase of elongation factor G on the ribosome. *Proc Natl Acad Sci U S A* **96**: 9586–9590.
- Romisch, K., Webb, J., Herz, J., Prehn, S., Frank, R., Vingron, M., and Dobberstein, B. (1989) Homology of 54K protein of signal-recognition particle, docking protein and two E.coli proteins with putative GTP-binding domains. *Nature* **340**: 478–482.
- Runnels, L.W., and Scarlata, S.F. (1995) Theory and application of fluorescence homotransfer to melittin oligomerization. *Biophys J* **69**: 1569–1583.
- Saraogi, I., Akopian, D., and Shan, S.O. (2014) Regulation of cargo recognition, commitment, and unloading drives cotranslational protein targeting. *J Cell Biol* **205**: 693–706.
- Shan, S.O., Stroud, R.M., and Walter, P. (2004) Mechanism of association and reciprocal activation of two GTPases. *PLoS Biol* **2**: e320.
- Shan, S.O., Chandrasekar, S., and Walter, P. (2007) Conformational changes in the GTPase modules of the signal recognition particle and its receptor drive initiation of protein translocation. *J Cell Biol* **178**: 611–620.
- Stjepanovic, G., Kapp, K., Bange, G., Graf, C., Parlitz, R., Wild, K., Mayer, M.P., and Sinning, I. (2011) Lipids trigger a conformational switch that regulates signal recognition particle (SRP)-mediated protein targeting. *J Biol Chem* **286**: 23489–23497.
- Valent, Q.A., Scotti, P.A., High, S., de Gier, J.W., von Heijne, G., Lentzen, G., et al. (1998) The escherichia coli

- SRP and SecB targeting pathways converge at the translocon. *EMBO J* **17**: 2504–2512.
- Van den Berg, B., Clemons, W.M., Jr., Collinson, I., Modis, Y., Hartmann, E., Harrison, S.C., and Rapoport, T.A. (2004) X-ray structure of a protein-conducting channel. *Nature* **427**: 36–44.
- Weiche, B., Burk, J., Angelini, S., Schiltz, E., Thumfart, J.O., and Koch, H.G. (2008) A cleavable N-terminal membrane anchor is involved in membrane binding of the escherichia coli SRP receptor. *J Mol Biol* **377**: 761–773.
- Wu, Z.C., de Keyser, J., Kedrov, A., and Driessen, A.J. (2012) Competitive binding of the SecA ATPase and ribosomes to the SecYEG translocon. *J Biol Chem* **287**: 7885–7895.
- Yosef, I., Bochkareva, E.S., Adler, J., and Bibi, E. (2010) Membrane protein biogenesis in Ffh- or FtsY-depleted escherichia coli. *PLoS One* **5**: e9130.
- Zelazny, A., Seluanov, A., Cooper, A., and Bibi, E. (1997) The NG domain of the prokaryotic signal recognition particle receptor, FtsY, is fully functional when fused to an unrelated integral membrane polypeptide. *Proc Natl Acad Sci USA* **94**: 6025–6029.
- Zhang, X., Schaffitzel, C., Ban, N., and Shan, S.O. (2009) Multiple conformational switches in a GTPase complex control co-translational protein targeting. *Proc Natl Acad Sci USA* **106**: 1754–1759.

Supporting information

Additional supporting information may be found in the online version of this article at the publisher's web-site.